Magnetic Moment of the Free Muon*†

T. COFFIN, R. L. GARWIN,‡ S. PENMAN, L. M. LEDERMAN, AND A. M. SACHS
Columbia University,§ New York, New York

(Received October 1, 1957)

The magnetic moment of the positive μ meson has been measured in several target materials by a magnetic resonance technique. Muons were brought to rest with their spins parallel to a magnetic field. A radio-frequency pulse was applied to effect a spin reorientation which was detected by counting the decay electrons emerging after the pulse in a fixed direction. Results are expressed in terms of a g factor which for a spin $\frac{1}{2}$ particle is the ratio of the actual moment to $e\hbar/2m_\mu c$. The most accurate result obtained in a $CHBr_3$ target, is that $g=2(1.0026\pm0.0009)$ compared to the theoretical prediction of $g=2(1.0012)$. Less accurate measurements yielded $g=2.005\pm0.005$ in a copper target and $g=2.00\pm0.01$ in a lead target.

I. INTRODUCTION

THE μ meson has often been described as one of the more baffling of elementary particles. It alone, among the unstable particles, has no strong interaction. Aside from its usefulness as a tool in the study of nuclear structure and the details of parity violation in weak interactions it appears to play no essential role in any organization of fundamental particles. A precise measurement of the magnetic moment of the muon offers some promise for clarification of this situation.

The Dirac equation predicts precisely 2 for the g value of a spin $\frac{1}{2}$ particle. Including corrections due to the interaction of the particle with its radiation field, one obtains[1,2]

$$g_\mu=2\left(1+\frac{\alpha}{2\pi}+0.75\frac{\alpha^2}{\pi^2}+\cdots\right) \quad (1)$$
$$=2(1.0012).$$

Deviations from this prediction may occur because of the structure and interaction properties of the μ meson. On the other hand, (1) provides a test of quantum electrodynamics in a heretofore unexplored domain. Whereas the major radiative corrections to the electron moment arise from virtual quanta of energy less than the electron rest mass, the meson moment correction involves virtual photons of 200 times the energy and hence wavelengths that are 200 times smaller than in the electron case. It has been pointed out[3] that the existence of a cutoff in quantum electrodynamics at an energy λ would alter the g value as follows

$$g=2\left\{1+\left[1-\frac{2}{3}\left(\frac{m_\mu}{\lambda}\right)^2\right]\frac{\alpha}{2\pi}+\cdots\right\}. \quad (2)$$

It might be remarked[4] that the model used in reference 3 implies a modification in the scattering of one Dirac particle by another. Such a modification can be described by a mean square radius, the appropriate relation being $\langle r^2\rangle_e=6(\hbar/\lambda c)^2$. Qualitatively, at least, the measured proton radius should constitute an upper limit for such an "electrodynamic radius." Hence the fractional alteration of the muon moment from such a presumed breakdown of quantum electrodynamics should not exceed $\sim0.02(\alpha/2\pi)$.

In the original meson parity experiment[5] it was established that the nonconservation of parity in the $\pi\rightarrow\mu+\nu$ decay leads to a high degree of polarization in the external μ meson beam of the Nevis cyclotron. This polarization was deduced from the spatial anisotropy in the parity nonconserving $\mu^+\rightarrow e^++\nu+\bar{\nu}$ decay, the electron direction being strongly correlated with the μ spin direction. In GLW the angular distribution of the emitted electrons was found to be $\sim1-0.3\cos\theta$. By counting the decay electrons in a given direction, a change in the μ spin direction can be detected. In the GLW experiment a small constant magnetic field, H, perpendicular to the μ spin direction, was set up in the target region. The rate of μ spin precession, given by $\omega=geH/2(m_\mu c)$, was detected by counting the decay electrons emitted at a given angle to the initial spin direction after a fixed time delay.[6] This first measurement of the spin precession rate indicated a g-value of 2.00 ± 0.02. A more accurate determination by a similar method reported a g value of 2.008 ± 0.014.[7]

A more precise method of measuring the magnetic

* This research is supported by the U. S. Atomic Energy Commission and the Office of Naval Research.

† A preliminary report of this work has been given in Phys. Rev. **106**, 1108 (1957).

‡ Also at International Business Machines Watson Laboratory.

§ A large fraction of the data utilized in this paper was obtained at the Carnegie Institute of Technology cyclotron at Saxonburg, Pennsylvania, which is also supported by the U. S. Atomic Energy Commission.

[1] A. Petermann, Nuclear Phys. **3**, 689 (1957).

[2] C. Sommerfeld, Phys. Rev. **107**, 328 (1957).

[3] Beresteskii, Krokhin, and Khlebnikov, J. Exptl. Theoret. Phys. U. S. S. R. **30**, 788 (1956); [translation: Soviet Phys. JETP **3**, 761 (1956)].

[4] N. M. Kroll (private communication).

[5] Garwin, Lederman, and Weinrich, Phys. Rev. **105**, 1415 (1957), hereafter referred to as GLW.

[6] Similar techniques have been employed for measuring nuclear moments. See *Beta- and Gamma-Ray Spectroscopy*, edited by K. Siegbahn (Interscience Publishers, Inc., New York, 1955). See also: M. Goldhaber, Phys. Rev. **101**, 1828 (1956).

[7] Cassels, O'Keefe, Rigby, Wetherell, and Wormald, Proc. Phys. Soc. (London) **A70**, 451 (1957).

moment is to employ a resonance technique in which an oscillating magnetic field is used to reorient the μ spin in a large static magnetic field. The fact that the muon is a charged unstable particle with an asymmetric decay pattern permits a technique that combines some of the features of bulk resonance and atomic beam techniques. The source strength of about 100 muons per second eliminates the possibility of any measurement that depends on absorption of energy from the oscillating field as in bulk resonance. The charge and high velocity of the muon prevents measurements on a moving particle as in atomic beam techniques, but the fact that the muon decays asymmetrically with a 2.2-μsec mean life permits a resonance measurement on individual particles that have been brought to rest in a target. The mean life, however, restricts the time available per measurement to $\sim 2\,\mu$sec thus setting a lower limit ($\Delta\omega\,\Delta t \geq 1$) on the sharpness of the resonance observed. The absolute uncertainty in frequency, $\Delta\omega$, due to the finite time available, Δt, is fixed, and hence the fractional line breadth is inversely proportional to the magnitude of the magnetic field at which the resonance is obtained.

In this experiment muons were brought to rest in a target with their spin polarized along a magnetic field, H. A pulsed rf magnetic field perpendicular to the fixed magnetic field was used to effect a reorientation of the muon spin. When the frequency of the rf field is equal to $g(eH/2mc)$, i.e., at resonance, the angle through which the muon precesses in time t is given by $\theta=\frac{1}{2}\int_0^t g(eH_1/2mc)dt$, where H_1 is the magnitude of the rf field. The factor $\frac{1}{2}$ in the expression for θ is due to the use of an oscillating rf field. This may be considered in the usual way as the sum of two counter rotating components, only one of which is effective (to first order). For a μ meson with a g value of 2, 180° rotation implies a pulse for which $\int_0^t H_1 dt=70$ gauss-μsec. The 180° rotation corresponds to the quantum-mechanical 100% transition probability between two states of opposite spin alignment, i.e., between $m_s=\pm\frac{1}{2}$ and $m_s=\mp\frac{1}{2}$. (Of course it is not possible by such an experiment to determine the absolute direction of the spin.)

The decay electrons emerging in the backward direction after the rf pulse was over were counted; the "peak" rate was obtained for no transition, a decrease in rate ("valley" rate) indicating that a magnetic transition had taken place.

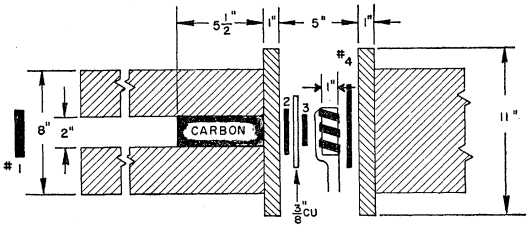

FIG. 1. Experimental arrangement.

II. EXPERIMENTAL ARRANGEMENT

A. Counting Electronics

The meson source used in these experiments was the "85-Mev" π^+ meson beam at the Nevis cyclotron and the "110-Mev" beam at the Carnegie Institute of Technology cyclotron. Momentum analysis was achieved with a steering magnet used to bend the beam away from its emergent direction. Since μ mesons of the same momentum as π mesons have a greater range, a relatively pure μ source was obtained by including before the target sufficient absorber to stop most of the π's.

Figure 1 shows the counting arrangement. A meson entering through a 2-in. hole in the magnet pole piece and stopping in the target is identified by a fast coincidence circuit which is actuated by pulses in counters 1, 2, and 3 together with an anticoincidence requirement on counter 4. The output of the $123\bar{4}$ circuit is used to initiate two operations. An rf pulse is applied to a coil wound around the target, and after a 2-μsec delay, a gate pulse 3 μsec long is formed.

Decay electrons emitted in the backward direction are counted by a $23\bar{1}\bar{4}$ circuit. Only $23\bar{1}\bar{4}$ pulses that fall within the gate interval are counted as "events." The ratio of "event" counts to "gate" counts is used to determine when a spin reorientation has taken place.

The anticoincidence requirement on counter number 1 for the $23\bar{1}\bar{4}$ coincidence serves to prevent the counting of incoming beam particles. The anticoincidence requirement on number 4 served as an additional discrimination against decay electrons from μ's that had entered the rear pole piece. Since only $23\bar{1}\bar{4}$ pulses that fall within the gate interval are counted as events, the function of the anticoincidence counters in $23\bar{1}\bar{4}$ is to reduce the number of accidental events to a negligible number, (<1%).

Figure 2 is a block diagram of the electronic equipment. The fast coincidence circuits are of a standard type and are followed by EFP60 pulse shaping circuits. The $123\bar{4}$ output is used to trigger the rf gate circuit. The 2-μsec delay for the gate is obtained by using RG 65 delay cable. In order to allow full recovery of the thyratron circuit in the rf pulser (see below) a dead-time circuit follows the pulse shaper. This insures a minimum interval of 200 μsec between counts fed to the rf generator.

Decay electrons which give rise to a coincidence output within the gate interval are detected in the final slow coincidence between the gate pulse and the $23\bar{1}\bar{4}$ output. The output from the slow coincidence circuit is scaled as "events." The number of gate pulses is also scaled. The resonance is indicated by a decrease in the number of events per gate. The total number of $23\bar{1}\bar{4}$ coincidences is also scaled as "ungated." The ratio of

ungated to gates is used during a run to check the counting circuit efficiencies.

B. Counters

The counters are constructed of $\frac{1}{4}$-in. plastic scintillator. Counters 1 and 2 are each 3-in.×3-in. Counter 3 has the same cross sectional dimensions as the target, 2-in.×2-in. This counter is kept small to reduce the background due to μ's stopping in the counter itself. Counter 4 is made large, 5-in.×5-in., to obtain maximum efficiency in rejecting particles which in passing through the target have scattered through large angles. Counters 2, 3, and 4 are mounted on 2-ft light pipes which serve to remove the photomultipliers from the magnetic field. The photomultipliers are magnetically shielded by a mu-metal sleeve and a $\frac{1}{4}$-in. iron tube. Counting rates were measured as a function of magnetic field with the absorber removed and the counter efficiency was proven to be independent of the magnetic field.

The photomultipliers are 6810's operated at from 2100 to 2600 volts and are capable in this arrangement of delivering 10-volt pulses into a 120-ohm load for the light available from a minimum ionizing particle.

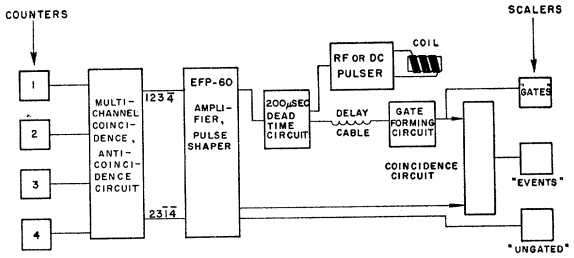

FIG. 2. Block diagram of the counting electronics.

C. rf Circuit

A phase-stable rf pulse of computable characteristics was obtained by ringing the resonant circuit formed by the target coil and its associated stray capacity. The circuit is shown in Fig. 3 together with a circuit for "dc pulsing" which will be described below. The initiating pulse is obtained from a $123\bar{4}$ coincidence. This triggers the EFP60 univibrator which, in this circuit, will deliver a 600-volt pulse with a 20-μsec rise time. The operating point of the tube is somewhat unusual but it was found that most EFP60's functioned without breakdown. The EFP60 pulse fires the 4C35 hydrogen thyratron which discharges condenser C_1 into the cathode of the normally cutoff 4C33. Thus a large current pulse is injected through the grounded grid into the anode tank circuit of the 4C33 for a short time compared to a cycle of the resonant circuit.

The 4C33 plate current pulse discharges C_2 putting a large negative voltage on the resonant circuit. The 4C33 is then cut off again by the discharge of C_1 permitting the cathode to rise, and the resonant circuit is free

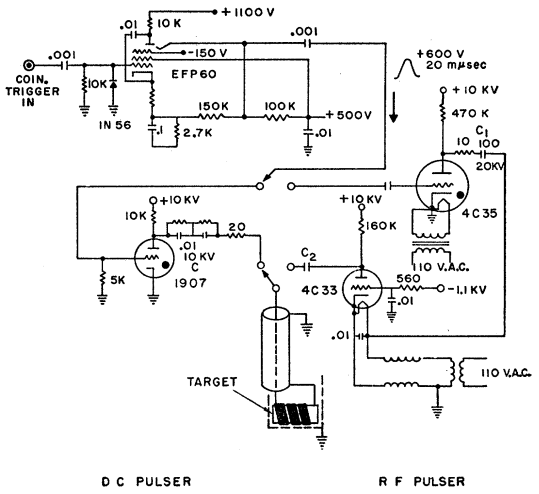

FIG. 3. Circuit diagram of rf and dc pulsers.

to respond to the voltage surge it has received. The electrostatic shielding by the grounded grid prevents reduction of the Q of the resonant circuit, which otherwise would be coupled capacitively through the tube to dissipative elements in the thyratron driver circuit. The damped oscillation has the form $Ae^{-\alpha t}\cos\omega t$ and the magnetic field in the region of the target is adjusted so that $\int_0^{t_1} Ae^{-\alpha t}dt = 70$ gauss-μsec, where t_1 is the time interval from the initiation of the rf pulse to the center of the gate pulse.

D. Magnet

For the runs at 7 and 16 Mc/sec, 8-in. diameter pole pieces were used, one of which had a 2-in. hole through its center. The large ratio of gap width (5 in.) to pole diameter and the presence of the hole resulted in a total field inhomogeneity of 0.8% over the $2\times2\times\frac{7}{8}$-in. target region. For the more accurate measurements at 22 Mc/sec, circular pole tips 11 in. in diameter and $\frac{3}{4}$ in. thick were added to the 8-in. pole pieces, the pole tip thickness serving as part of the absorber between counters 1 and 2. There were also adjustable rings $\frac{3}{4}$-in. long and $\frac{3}{8}$-in. in radial thickness around the circumference of the pole tips. The shimming procedure consisted of obtaining the most homogeneous field possible by moving the adjustable rings and then performing fine adjustments with steel shim stock fastened to the rear pole tip. The total field variation over a 2-in. diameter circular region, $\frac{7}{8}$ in. thick, was held to 0.08%. The target material was confined to this region by the Teflon insert described below.

In the mapping of the field and in the subsequent monitoring, a nuclear magnetic resonance probe was fastened to a rigid arm which was mounted on a milling machine bed. Precise and reproducible motion of the probe was thus achieved.

At a field of 1800 gauss the magnet required about 7 amperes of current. A feedback series current regulator

incorporating 2N278 transistors was used.[8] The error signal for the regulator is taken from a type K potentiometer measuring the voltage across a current shunt in series with the magnet. The current is thus adjusted by changing the setting on the potentiometer. The regulator held the current variation to $<0.002\%$ when used with an automobile storage battery source during the interval of a single run (15 min).

E. Target

The target assembly consists of a Lucite frame, 5-in.×5-in. which clamps onto an aluminum spacer held between the magnet pole pieces. The Lucite frame holds a box made of $\frac{1}{32}$-in. Micarta on which the three-turn rf coil is wound. The whole assembly is wrapped in Styrafoam and aluminum foil for insulation against 30 kv and for rf shielding. The liquid and powder target materials were held in a rectangular container $2\times2\times\frac{7}{8}$-in. which could be easily inserted into the target assembly. For the runs at 22 Mc, a maximum field homogeneity was desired. Since the field variation was greatest in corners of the target container, a Teflon insert was added which restricted the effective target area to a 2-in. diameter circular region. Because of the comparatively low density of Teflon, relatively few muons stopped in the corners and most of these were depolarized before decaying. The Micarta target holder contained a stop so that the target container could be positioned accurately, and a pickup loop was mounted for monitoring the rf pulse. The entire target assembly with cup empty contributed a background of $\sim30\%$ of the rate.

The target material had to fulfill four principal requirements. It should (a) have sufficient density to stop a large fraction of the μ's, (b) not depolarize μ's in the dc experiment, (c) allow the rf field to penetrate the target volume, and (d) have no *large* internal fields to shift or broaden the resonance line.

An initial trial run using polyethylene as a target material yielded a very broad shallow resonance line. Since polyethylene yielded a large dc effect it was concluded that the muons were not depolarized but that local magnetic fields were broadening the resonance line as in the case of the proton line in nuclear magnetic resonance measurements of polyethylene. The subsequent runs that were made with a view towards high precision used a liquid target, since the molecular collision times are such that local fields more effectively average to zero. The liquid used was bromoform, $CHBr_3$, which has a density of 2.89 g/cm^3 and was readily available. Metals to be used as target materials, had to be in a suitable form for use in an rf field. The copper was electrolytic dust with a grain size which was small compared to the skin depth at 22 Mc/sec. The lead was in the form of a 95% lead, 5% polyethylene emulsion. Nothing was known about the size of the lead domains other than could be deduced from the behavior of the material as a target. Since the effect on the target coil Q was small and the rf was effective in flipping muon spins, it was assumed that the lead domains were very small compared to the skin depth.

[8] R. L. Garwin, Rev. Sci. Instr. (to be published).

III. EXPERIMENTAL PROCEDURE

A. Differential Range Curve

The initial step in setting up the resonance apparatus is the determination of the optimum amount of absorber to be placed between counters 1 and 2. Differential range curves were obtained by placing a $\frac{1}{8}$-in. copper plate between counters 3 and 4 and recording the ratio of $123\bar{4}$ coincidence counts to 12 coincidence counts as the absorber between 2 and 3 was varied. Three-eighths in. of copper is placed between 2 and 3, to reduce background. The proper amount of carbon is then inserted in the hole in the magnet pole piece so that the total is sufficient to place the target at the proper point on the range curve.

B. dc Pulser

Before actual resonance measurements were made, it was desirable to precess muons in order to observe the "peak-to-valley" ratio. This was done, for example, in testing various target materials for muon depolarization, in checking for excessive pion contamination and as a final check of the counters and electronics. A nonresonant spin-flipping arrangement was designed which made use of the same target coil and transmission line. In this procedure the longitudinal field of the large magnet is turned off and the muons are caused to precess by means of a 35 gauss-μsec direct-current pulse, which in about $\frac{1}{2}$ μsec effects a 180° spin rotation. Compared to the steady dc precession field employed previously in the GLW experiment, this has the advantage of permitting the use of a longer counting time interval after the pulse, since the muons are then stationary in their new orientation. The circuit is shown in Fig. 3. The EFP60 univibrator triggers the hydrogen thyratron causing C to discharge through the target coil. Enough damping is included to prevent ringing.

C. Observation of the Resonance Line

The procedure used in tracing out a resonance line was as follows. The rf frequency was first measured as described below. Because of the comparative difficulty in measuring the frequency of the pulsed rf it was left fixed during a run and the magnetic field used as the variable. A series of magnetic field settings was estimated (using $g\approx2$) so as to best define the line center. The required readings on the proton resonance probe were corrected for the difference in field between the target center and a standard monitor position adjacent to the target. This difference of 0.14% was checked periodically and at several magnetic field strengths and

remained constant. The magnetic field was then set to the desired value by setting the proton resonance oscillator at the corresponding frequency as determined by zero beating with a crystal-calibrated frequency meter (U. S. Navy type CKB 74028) and adjusting the magnet current until the resonance was observed. A typical run would last 15 minutes, after which the proton resonance frequency was redetermined. Repeatability was about 0.002%, which includes any possible drift in the magnetic field. The average counting rate was 2500 gate-counts per minute which yielded about 60 events per minute. Several measurements were made at each value of magnetic field during a run and points were taken on alternate sides of the resonance so as to minimize the effect of possible long-term counting efficiency drifts on the apparent line center.

D. Frequency Measurement

The measurement of the center frequency of the 1.5-μsec rf pulse to the required accuracy posed some difficulty due to the large band width intrinsic in the pulse duration. In the early measurements, the spectrum of the triggered rf was Fourier-analyzed by using a General Radio wave meter type 805-C. After recording the rf line shape, the wave meter was set to the dial reading corresponding to the rf spectrum center, and its own frequency response was then measured with a GR signal generator to determine the frequency corresponding to the dial setting. The GR signal generator was then zero beat with the crystal-calibrated frequency meter. The method was time-consuming and limited in accuracy. For the last and most accurate set of measurements at 22 Mc/sec, a method resembling a direct beat-frequency measurement was used.

A sample of the rf pulser output, obtained from a pickup loop near the target coil, is mixed with the output of the GR signal generator which is adjusted to be several times the amplitude of the induced rf pulse. The rf pulser is triggered at about a 100 cps rate. The resultant signal is rectified and the envelope displayed on an oscilloscope with long persistence screen. The sweep is triggered simultaneously with the rf pulser. The mixed signal form before detection has the wave form

$$V_{\text{in}}=B\cos\omega' t+Ae^{-\alpha t}\cos(\omega t+\phi), \qquad (1)$$

where ω'=signal generator frequency, ω=pulser frequency, $1/\alpha$=decay time of the rf pulse (1.5 μsec), and ϕ is a phase factor which is arbitrary since the rf pulser is triggered randomly with respect to the generator phase.

For simplicity we shall discuss a square law detector although a linear detector was used. The envelope displayed on the oscilloscope face has the form

$$V_{\text{out}}{}'=B^2+A^2e^{-2\alpha t}+2ABe^{-\alpha t}\cos(\phi+\Delta\omega t), \qquad (2)$$

where $\Delta\omega=\omega-\omega'$. When $\Delta\omega=0$, i.e., the frequency generator is set correctly, a family of curves corresponding to the various values of ϕ are seen. As can be seen from the functional form of Eqs. (1) or (2), there can be no crossing of curves for different values of ϕ in this case. However, if $\Delta\omega$ is not equal to zero the curves seen on the oscilloscope face will cross since a point (V,t) at total phase ψ can be on two curves, one with $\phi_1=\psi-\Delta\omega t$ and the other with $\phi_2=-\psi-\Delta\omega t$. For one of these, ψ is increasing, for the other, ψ is decreasing; therefore, the curves cross. The signal generator is tuned until no crossings are seen. The signal generator frequency is then measured with the same crystal calibrated frequency meter used in the magnetic field measurements. The accuracy of the frequency measurement is determined by the time available before the rf pulse has decayed excessively, or about 2 time constants (3 μsec) in the above arrangement. Figure 4 shows photographs of the oscilloscope screen for indistinguishable frequencies and for a frequency difference of 0.04%. The reproducibility was found to be about $\pm$0.01% and the method has no bias if the adjustments are made with both increasing and decreasing frequency. In the course of the run, the rf frequency was checked periodically by at least two observers. Long-term drifts during the course of a run amounted to less than 0.02%.

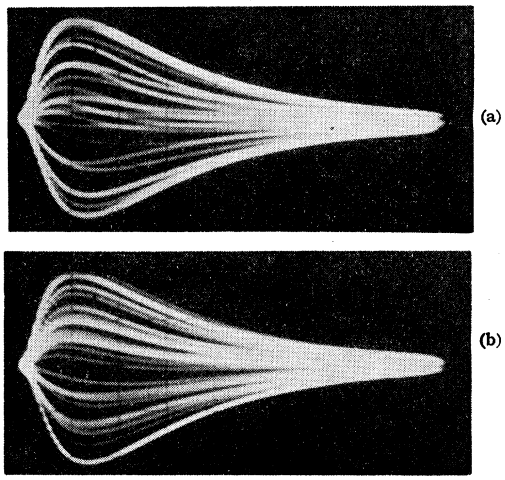

FIG. 4. Photographs of oscilloscope screen during frequency measurement. The top photograph is for a frequency difference of 0.04%. The bottom one is for indistinguishable frequencies.

ANALYSIS OF DATA

A. Line Center

The resonance experiment was performed at 7, 16, and 22 Mc/sec using bromoform, copper dust, and lead-polyethylene targets.

In the most accurate measurements, i.e., those made at 22 Mc/sec, there were 5 useful runs made with the bromoform target. Since these were made at slightly different frequencies, the line center was determined for each run separately and the quoted result is the weighted average of these determinations.

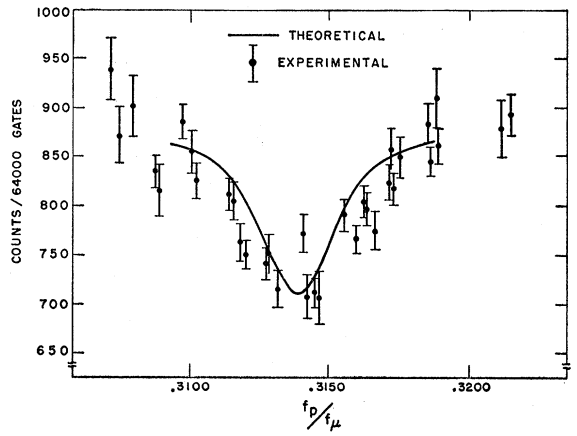

FIG. 5. Theoretical line shape and composite of the experimental points.

Figure 5 shows a theoretical curve for the resonance line computed for an rf amplitude corresponding to 100% transition probability. This curve and a number of others for different rf amplitudes were calculated numerically on the IBM 650 computer by integrating the differential equations for the expectation value of the muon spin in the presence of the dc field and the exponentially-decaying rf field. The deviation of the counting rate from its off-resonance value is simply proportional to the change of the z-component of the muon spin, so that after normalization to the same amplitude, the theoretical and experimental curve should be identical. Also shown is a composite of all the data points used in determining the line center. This composite was prepared by shifting the rf frequency to a common value and normalizing the "peak-to-valley" ratio of the various runs. Figure 5 indicates that the experimental points fall on a broader curve than the calculated one, suggesting possible effects of rapidly varying local fields.

A statistical uncertainty of 2% to 3% is associated with each point on a resonance curve. The best method of determining the line center would be to perform a least-squares fit of a theoretical line shape to the data points. Since the agreement of the experimental points with the calculated theoretical curve is not good, a determination of the line center has been made assuming only that the line is symmetric.

Two simple arbitrary symmetric curves were fitted to the data points of each run by using a least-squares criterion. One curve was simply two straight lines of opposite slope fit to points in a region of the resonance curve where the slope is steep. The depth of the curve was selected visually and the point of intersection and the slope were varied so as to minimize the quantity $M=\Sigma_i(\delta_i/\epsilon_i)^2$, where δ_i is the difference between an experimental point and the value of the theoretical curve at the same field, ϵ_i is the statistical uncertainty associated with the experimental point, and the summation is taken over all experimental points in the relevant region. The other curve was a Gaussian of the form $A-B\exp[-(f_p-f_0)^2/C]$. A is the average of the off-resonance counting rate. Two of the parameters, B and C, were selected to give a best visual fit to the composite of data points in all of the runs. The curve center, f_0, was varied so as to minimize the quantity M. The line centers determined by the two methods agree to 0.03%. Table I presents the results of each of the five runs made with bromoform at 22 Mc/sec in terms of the ratio of the muon frequency f_μ to proton frequency f_p at the value of the magnetic field corresponding to the resonance curve center. The ratios quoted are in each case the average of the results of two methods of determination.

Table II lists the results of earlier runs made in bromoform, lead, and copper at lower frequencies, as well as one run made in copper at 22 Mc/sec. Since the uncertainty in these measurements was greater than those in Table I, the line-center analysis was less detailed and consisted of only visual fits of straight lines to the data.

ERRORS

The greatest source of uncertainty in the experimental results stems from the statistical errors associated with each experimental point, resulting in an uncertainty in the determination of the line center. The standard deviations quoted in Table I were estimated from the least-squares analysis.

The error from a possible undetected drift in counting-circuit efficiency was minimized by taking points consecutively on opposite sides of the resonance line center. Since every point was measured several times, long-term drifts would have been detected. The extreme assumption of a 5% drift over the period of a run results in a shift in the line center that is about 0.01% and hence has been neglected.

The experimental method employed here did not require a primary frequency standard. The result is expressed as a ratio of the applied rf frequency to the proton resonance frequency in the magnetic field corresponding to the muon resonance line center. Both frequencies were measured with the same crystal-calibrated frequency meter. Thus the ultimate standard is the proton moment. The rf frequency measurement, f_μ, (described above) was reproducible to 0.02%, the proton resonance frequency, f_p, to much better than

TABLE I. Results of measurements made in $CHBr_3$ at 22 Mc/sec.

Run	f_μ (kc/sec)	f_p (kc/sec)	f_μ/f_p
1	22770±2	7153±11	3.1833±0.0050
2	22769±2	7146±11	3.1862±0.0050
3	22763±2	7142±11	3.1869±0.0050
4	22741±2	7133±11	3.1881±0.0050
5	22600±2	7089±11	3.1882±0.0050
		Average	3.1865±22

0.01%. Uncertainties due to drift in the magnetic field between points (~15 min) and in the rf during a resonance run were negligible. The largest error in the magnetic field determination was contributed by the field inhomogeneity over the region of the sample and the uncertainty in the positioning of the sample relative to the field map. This possible error is estimated to be less than 0.01%. Proton resonance measurements in organic liquids indicate that the correction due to diamagnetism in the target material is less than 0.0005%. The Block-Siegert correction is less than 0.01%.

The errors discussed above are independent and were compounded in quadrature and are given in Table I. Averaging the results from the 5 runs gives a value of $f_\mu/f_p=3.1865\pm0.0022$. The quantity of most interest is the g factor of the muon. This involves the muon mass in the following way

$$g_{\mu^+}=\left(\frac{m_{\mu^+}}{m_p}\right)\left(\frac{f_{\mu^+}}{f_p}\right)g_p,$$

where m_{μ^+} is the muon rest mass, m_p is the proton mass, and g_p is the proton g factor. We take $g_p=2.7927$ and $m_p=1863.1m_e$.[9]

The muon mass has recently been discussed by Crowe[10] whose results utilized principally the data from the π- and μ-mesonic x-ray,[11] momentum and emulsion range momentum and pion capture in hydrogen to obtain pion masses, $\pi-\mu$ mass difference, and muon masses.

Crowe finds

$$m_\mu=206.86\pm0.11m_e,$$

which yields

$$g_\mu=2(1.0026\pm0.0009). \quad (3)$$

This result is about one and one-half standard deviations higher than the electrodynamic prediction 2(.0012), of Eq. (1).[12] A lower limit to the muon mass from x-ray measurements is[11]

$$m_\mu>206.77\pm0.03m_e.$$

Using this limit, we find

$$g_\mu>2(1.0021\pm0.0007). \quad (4)$$

Another way of utilizing these results is to assume the validity of quantum electrodynamics to second order and use the f_{μ^+}/f_p ratio to derive the muon mass. This yields

$$m_{\mu^+}=206.58\pm0.14. \quad (5)$$

TABLE II. Results of measurements made in copper, lead, and at lower frequencies in $CHBr_3$.

Target material	Frequency (Mc/sec)	g value
Pb (in plastic)	16	2.00 ±0.01
Cu-(dust)	16	2.02 ±0.01
Cu-(dust)	22	2.005 ±0.004
CH_2	7.5	2.01 ±0.01
$CHBr_3$	7.5	2.00 ±0.01
$CHBr_3$	16 (3 runs)	2.0064±0.0048

CONCLUSIONS

The g value of the positive muon, arrested in liquid bromoform has been determined with a precision of 0.09%. No large variations in g value have been observed among bromoform, Cu, and Pb, and therefore it seems reasonable to assume that the positive muon is "free" in these materials.[13] The closeness of the result to the predictions of the Dirac equation with radiative corrections establishes more firmly the character of the muon as a "heavy electron" and intensifies the problem of the muon-electron mass difference.

A more accurate determination of the muon moment is in progress which will utilize a frequency of 100 Mc/sec and hence increase the precision by a factor of 5. However, a better test of the radiative corrections to the moment depends on a more accurate mass determination. An alternative method consists of measuring directly the departure of the g value from 2. Research along this line is being conducted at several laboratories at the present time.

ACKNOWLEDGMENTS

The authors wish to thank Professor N. M. Kroll for helpful discussions.

A substantial fraction of this work was carried out with the aid of the 450-Mev cyclotron of the Carnegie Institute of Technology. We are most grateful to Professor R. Sutton and the Carnegie Institute staff for their generous hospitality and assistance in making available to us the excellent facilities of the Nuclear Research Center in Saxonburg, Pennsylvania.

We also acknowledge the assistance of Mr. Warner Hayes for the runs at Saxonburg.

[9] Cohen, DuMond, Layton, and Rollett, Revs. Modern Phys. **27**, 363 (1955).

[10] K. Crowe, Nuovo cimento **5**, 541 (1957).

[11] Koslov, Fitch, and Rainwater, Phys. Rev. **95**, 291 (1954).

[12] In the use of mesonic x-ray data on the muon mass, it will be recalled that these include a substantial (0.4%) correction due to vacuum polarization. See E. Wichmann and N. M. Kroll, Phys. Rev. **96**, 232 (1954); L. Foldy and E. Eriksen, Phys. Rev. **95**, 1048 (1954); A. Mickelwait and H. C. Corben, Phys. Rev. **96**, 1145 (1954).

[13] The Knight shift in the metals is expected to be below our present accuracy, being less than that common to nuclei because of the smaller density of conduction electrons at the muon. This would be true even though the muon moment is considerably larger than ordinary nuclear moments, unless the conduction electrons had very predominantly p character about the nuclei.

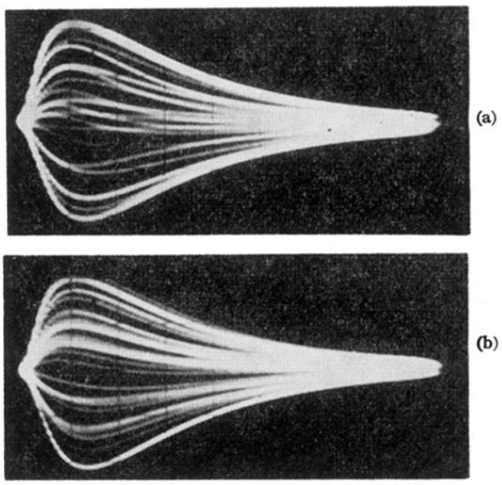

FIG. 4. Photographs of oscilloscope screen during frequency measurement. The top photograph is for a frequency difference of 0.04%. The bottom one is for indistinguishable frequencies.